

# FUNCTIONAL AND STRUCTURAL EFFECTS OF NONDAMAGING RETINAL LASER THERAPY FOR MACULAR TELANGIECTASIA TYPE 2

## A Randomized Sham-Controlled Clinical Trial

DANIEL LAVINSKY, MD, PhD,\*† MONICA OLIVEIRA DA SILVA, MS,\*† ANNE E. CHAVES, MD,\*† WAGNER F. M. SCHNEIDER, MD,\* FABIO LAVINSKY, MD, PhD,† DANIEL PALANKER, PhD‡§

**Purpose:** Macular telangiectasia (MacTel) Type 2 is a progressing neurovascular disease of the macula, currently lacking effective treatment. This study assessed the effect of nondamaging retinal laser therapy (NRT) compared with sham.

**Methods:** Twelve MacTel patients were enrolled in this double-masked, controlled, randomized clinical trial. For the nine patients with both eyes eligible, one eye was randomized to NRT or sham and the other received alternate treatment. For three patients with only one eye eligible, that eye was randomly assigned either NRT or sham. Ellipsoid zone disruption, best-corrected visual acuity, and macular automated perimetry at 12 months served as structural and functional measures.

**Results:** Eleven eyes were randomized to sham and 10 to NRT. Baseline best-corrected visual acuity was 66 letters (20/50) for sham and 72 letters (20/40) for NRT ( $P = 0.245$ ). Ellipsoid zone disruption area was  $298 \mu\text{m}^2$  in sham and  $368 \mu\text{m}^2$  in NRT ( $P = 0.391$ ). At 12 months, ellipsoid zone disruption increased by 24% in sham and decreased by 34% in NRT ( $P < 0.001$ ). Best-corrected visual acuity measures remained stable during follow-up compared with baseline. At 1 year, the mean macular sensitivity was 28 dB in the NRT group, compared with 26 dB in sham.

**Conclusion:** Nondamaging retinal laser therapy was safe and well tolerated in patients with MacTel and resulted in structural and functional improvements, which could represent a protective effect of laser-induced hyperthermia. Longer follow-up and larger number of patients should help corroborate these effects.

RETINA 00:1–8, 2020

Macular telangiectasia (MacTel) Type 2 is a bilateral, slowly progressive, degenerative disease that affects the central macular region, resulting in visual distortion and central visual loss in late stages

caused by foveal atrophy or neovascular changes.<sup>1</sup> Because of the presence of telangiectatic vessels mainly on the temporal juxtafoveal region, it was initially described as a vascular disease. However, recently, it has been considered a neurodegenerative condition that affects Müller cells and retinal blood vessels and later causes loss of photoreceptors.<sup>2</sup>

There is no approved treatment for MacTel, although several approaches have been tried in small clinical trials, such as steroids, photodynamic therapy, laser photocoagulation, and anti-vascular endothelial growth factor therapy. No treatment to date has been able to halt visual loss progression or reverting the neurovascular degeneration.<sup>3–10</sup> Recently, a Phase 2

From the \*Department of Ophthalmology, Federal University of Rio Grande, Do Sul, UFRGS, Porto Alegre, Brazil; †Retina and Vitreous Research Center, Hospital de Clinicas de Porto Alegre, Porto Alegre, Brazil; and ‡Department of Ophthalmology, Stanford University, Stanford, CA. §Hansen Experimental Physics Laboratory, Stanford University, Stanford, CA.

None of the authors has any financial/conflicting interests to disclose.

Reprint requests: Daniel Lavinsky, MD, PhD, Quintino Bocaiuva 673, Moinhos de Vento, Porto Alegre, RS Brazil 90440-051; e-mail: Daniellavinsky@gmail.com

randomized clinical trial of a surgical implant of the ciliary neurotrophic factor (CNTF) demonstrated slowing retinal degeneration progression as measured by loss of the ellipsoid zone (EZ) band on optical coherence tomography (OCT).<sup>11</sup>

We have previously reported an algorithm for photothermal laser therapy that adjusts laser power and duration based on Arrhenius integral.<sup>12</sup> The Endpoint Management algorithm maps a clinically relevant range of calculated Arrhenius integral values to linear steps in pulse energy, normalized to a titration dose for producing a particular laser endpoint. For clinical use, 30% energy setting in the Endpoint Management algorithm is used, with titration to a barely visible lesion. At these settings, nondamaging retinal laser therapy (NRT) caused retinal pigment epithelial (RPE) cells to respond to thermal stress by expression of heat shock proteins (HSPs) in vivo and also upregulation of glial fibrillary acidic protein expression that could represent Müller cells' activation and participation in wound contraction.<sup>12–15</sup>

These experimental findings suggest that NRT could be useful for treating MacTel Type 2, either by sublethal thermal stress that causes HSP upregulation in the RPE and photoreceptors or by Müller cell activation and stimulation of the tissue repair. Therefore, this study was designed to assess the safety and clinical effect of NRT in MacTel Type 2 patients compared with the sham laser.

## Methods

This randomized, double-masked, sham-controlled clinical trial was conducted at Hospital de Clinicas de Porto Alegre (HCPA) at Federal University of Rio Grande do Sul. The protocol was reviewed and approved by the Ethics and Research Committee of HCPA adhering to the tenets of the Declaration of Helsinki, and each subject gave written informed consent to participate in the study. This study is listed at [www.clinicaltrials.gov](http://www.clinicaltrials.gov) (NCT01975103).

### Participants

Eligible patients with the following inclusion criteria were enrolled: above 18 years of age, diagnosis of MacTel Type 2 with dilated vessels having characteristic juxtafoveal leakage on fluorescein angiography, clinical features such as crystalline deposits, right angle vessels, retinal opacification, and focal hyperpigmentation, and OCT findings such as inner or outer retinal cavitations and EZ break. Exclusion criteria included other causes of macular disease, any signs of neovascular disease, and insufficiently clear media for good

quality imaging. Eligible eyes had EZ disruption (EZD) smaller than 4 mm<sup>2</sup>, as measured by enface swept-source OCT (SS-OCT) imaging. Best-corrected visual acuity (BCVA) had to be better than 20/400 and worse than 20/40, as measured by the ETDRS protocol.

### Treatment Randomization and Masking

Eligible patients were assigned to receive NRT or sham laser, and both eyes of participants could be included. Participants with one study eye that met the inclusion criteria were randomized (1:1) to receive NRT or sham in the study-eligible eye. If both eyes were eligible, the right eye would be randomized (1:1) to receive NRT or sham and the left eye would receive the alternative treatment. Study eyes were treated with same parameters every 6 months and assessed on Day 0, Week 1, and Months 1, 3, 6, 9, and 12. Assignment was performed based on a simple randomization using a table of computer-generated random numbers concealed in opaque envelopes. Measurements of BCVA were obtained using ETDRS charts and standardized procedures by certified, masked visual acuity examiners without references to the patient's chart or history. A different masked investigator performed OCT and ophthalmologic examinations. Double masking was achieved by performing the same procedures as the active laser group but treating with zero therapeutic power in the sham group.

### Evaluation Procedures

Baseline examination included ETDRS BCVA, slit-lamp examination of the anterior segment, indirect ophthalmoscopy, color fundus photography, fluorescein angiography, and fundus autofluorescence using the Triton Plus system (Topcon, NJ).

Optical coherence tomography was performed using the recently introduced SS-OCT.<sup>16–18</sup> Baseline macula and choroidal thickness were obtained using 12 × 9-mm scan protocol and OCT angiography, whereas enface images were acquired using the 6 × 6 protocol. Same parameters were used for Day 0, Week 1, and Month 1, 3, 6, 9 and 12 assessments. Measurement of the EZD area was performed by masked, trained investigator using 6-mm × 6-mm scan volume with automatic segmentation for the outer retina, which comprises the inner plexiform layer/inner nuclear layer to the Bruch membrane, and individual B-scans were interpolated to manually detect the boundaries of EZD and measure the total area in μm<sup>2</sup>.

Functional retinal sensitivity was measured with fundus automated perimetry (CENTERVUE COM-PASS), using the macular protocol (10-2) (Figure 1). Examination was performed by an experienced masked technician with eye-tracker and autofocus features enabled. Foveal, inner ring and outer ring sensitivity

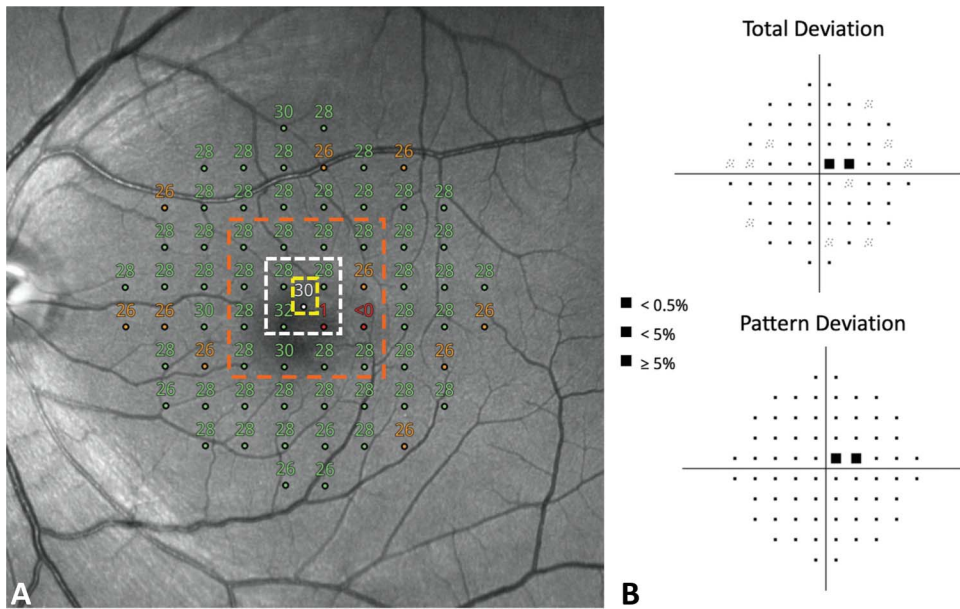


**Fig. 1.** A. Fundus automated perimetry at 12 months measured using the macular protocol. It shows central foveal sensitivity in decibels (dB) (yellow square), inner ring (white square), and outer ring (red square). B. Total and pattern deviation are presented, and data are compared with the normal population.

(decibels [dB]), and fixation area were measured at the 12-month visit using the same protocol by a masked technician. Inner ring sensitivity was obtained by averaging four points surrounding the central fixation area, which was defined as foveal sensitivity (nasal superior, nasal inferior, temporal superior, and temporal inferior), and the outer ring was the average of 12 measurements surrounding the inner ring. The structural correlation was obtained by infrared imaging acquired simultaneously.<sup>19</sup>

#### Laser Treatment Settings

PASCAL laser (Topcon) with 577 nm wavelength and 200- $\mu\text{m}$  retinal spot size was applied through Area Centralis HD contact lens (Volk Optical, Mentor, OH). Retinal treatment begins with titration of laser power to a minimally visible retinal lesion outside vascular arcades at 3 seconds, as reported previously.<sup>12</sup> Pulses of 15 ms have been used for titration, where pulse energy corresponding to a minimally visible burn was assigned as 100% energy on Endpoint Management settings, and energy was then set to 30% for treatment using the round macular grid pattern ( $r_{\text{in}} = 500 \mu\text{m}$ ,  $r_{\text{out}} = 3000 \mu\text{m}$ ) with 0.25-diameter spacing between the spots and additional  $3 \times 3$  patterns.<sup>14</sup> Laser patterns covered both the damaged and nondamaged retina in the posterior pole, as determined by OCT enface imaging. Sham treatment was applied with the same protocol as NRT; however, laser power was set to zero, so patients were able to see aiming beam in the pattern, but no actual therapeutic laser was used. Patients in both NRT and sham groups were treated every 6 months with the same protocol.

#### Outcome Measures

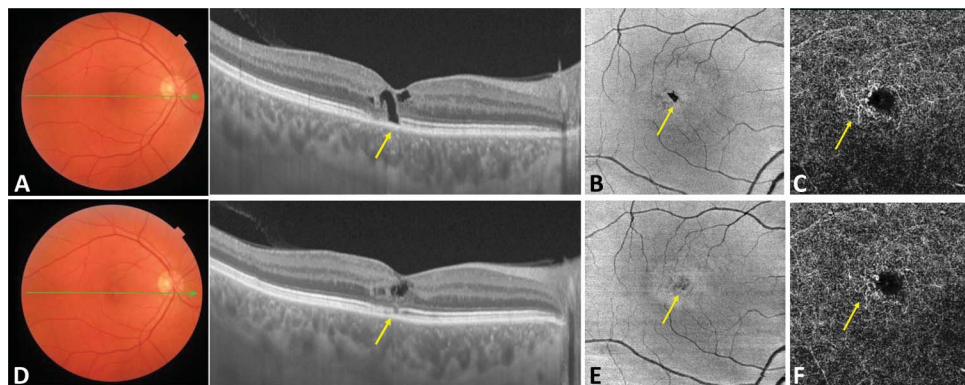
The primary outcome was change in the area of the EZD at 12 months, compared with baseline, measured by enface imaging using SS-OCT, as illustrated in Figure 2. Secondary outcomes were change in central macular thickness (CMT), central choroidal thickness measured on SS-OCT, BCVA at 12 months, compared with baseline, and difference in retinal sensitivity (dB) between NRT and sham groups at 12 months, using automated fundus perimetry. Safety assessment was performed every visit, and signs of macular scarring, central scotoma, or any other adverse collateral effect would be documented and reported.

#### Statistical Analysis

To address the intereye correlation and inclusion of either both or only one eye of a patient, the generalized estimating equation model was used. Adjustment for multiple pairwise comparisons was performed using the Bonferroni test, when effect was compared in multiple time points of the study. All statistical analyses performed by SPSS Software (IBM SPSS Statistics for Windows, Version 25.0. Armonk, NY: IBM Corp.). All clinical data were reported as adjusted mean  $\pm$  SE. Because of the limited number of cases and large variability in the baseline EZD area, measurements within groups were normalized to baseline data, and relative decrease or increase in the total EZD area (in %) was reported. A *P* value less than 0.05 was considered statistically significant.



**Fig. 2.** Color fundus image and high-resolution SS-OCT of the retina before the treatment (A), the corresponding enface image with the EZD zone (arrow) (B), and OCT angiography (C) showing the telangiectatic vessels on the superficial plexus (arrow). Corresponding images 1 year after the NRT demonstrate reduced EZD zone (arrow) in (D and E) and a discrete reduction in telangiectatic vessels on the superficial plexus (arrow) (F).



**Results**

*Study Participants and Baseline Characteristics*

Fourteen patients were screened from 2017 to 2018, and 12 were eligible for this study (mean age  $61 \pm 7.1$  years). Two patients were not eligible because of low visual acuity and larger than  $4 \text{ mm}^2$  EZD area on enface OCT measurement. Of 12 patients enrolled, 11 eyes were randomized to sham treatment and 10 eyes to NRT. Eleven patients were white (91%), with three men (25%) and nine women (75%). Three patients had only one eye eligible and were randomized to either NRT or sham. Reasons for ineligibility of the fellow eye were the presence of neovascularization in one eye, presence of a macular scar from previous posterior uveitis, and larger than  $4 \text{ mm}^2$  EZD area. Every patient completed the 12-month visit; however, one patient missed visits at Months 6 and 9 but returned for the last visit. An average of  $322 \pm 34$  laser spots was applied using macular grid and additional  $3 \times 3$  patterns, and mean power for the 100% titration burn was  $140 \pm 8.7$  mW. At baseline (Table 1), the mean BCVA was  $66.3 \pm 3.6$  letters for sham (20/50) and  $72.5 \pm 3.2$  letters (20/40) for NRT eyes ( $P = 0.24$ , 95% CI  $-16.65$  to  $4.25$ ), and EZD area was  $298 \pm 104 \mu\text{m}^2$  for sham and  $368 \pm 116 \mu\text{m}^2$  in the NRT group ( $P = 0.391$ ).

*Primary Outcomes*

*Ellipsoid zone disruption area.* Ellipsoid zone disruption area decreased significantly over time in the NRT group ( $-82.75 \pm 26 \mu\text{m}^2$  compared with baseline  $P = 0.029$  for 95% CI  $-161.06$  to  $-4.44$ ) and, although values increased in the sham group, there was no statistically significant change compared with baseline ( $60.69 \pm 35 \mu\text{m}^2$   $P = 1.0$  for 95% CI  $-42.19$  to  $163.56$ ). At 12 months (Figure 3), there was a significant difference in relative EZD comparing both groups with an increase of 24% in the sham group ( $1.24 \pm 0.11$ , 95% CI  $1.02$ – $1.46$ ) and a decrease of 34% in the NRT group ( $0.66 \pm 0.07$ , 95% CI  $0.53$ – $0.80$ ,  $P < 0.001$ ).

*Secondary Outcomes*

*Central macular and choroidal thickness and optical coherence tomography angiography.* There were no statistically significant changes in the CMT over the follow-up of the study, within groups or between them, with the mean CMT at 12 months of  $266.38 \pm 4.62$  for sham compared with  $269.78 \pm 4.71 \mu\text{m}$  for NRT ( $P = 0.1$ ) (Figure 4). The sham group had a nonsignificant decrease of  $2.1 \pm 0.81 \mu\text{m}$  from

Table 1. Baseline Characteristics

Baseline Characteristics	Treatment Group		P
	Sham	NRT	
Eyes	11	10	
Age (range)	62 (49–72)	62.5 (56–72)	
Gender	Male (2) Female (9)	Male (2) Female (8)	
Ethnicity	White (10) African (1)	White (9) African (1)	
BCVA (letters)	$66.3 \pm 3.6$ (20/50)	$72.5 \pm 3.2$ (20/40)	0.24
CMT ( $\mu\text{m}$ )	$268.49 \pm 4.63$	$270.42 \pm 4.57$	0.23
Central choroidal thickness ( $\mu\text{m}$ )	$245.01 \pm 18$	$251.89 \pm 20$	0.54
EZD area ( $\mu\text{m}^2$ )	$298 \pm 104$	$368 \pm 116$	0.39

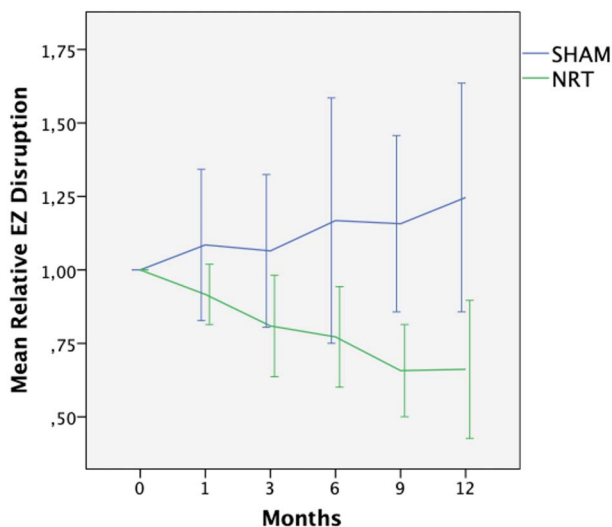


Fig. 3. Mean relative EZD area in NRT and sham groups over 12-month follow-up. Data were normalized by the baseline EZD area ( $\mu^2$ ).

baseline (95% CI  $-4.49$  to  $0.27$   $P = 0.14$ ) compared with NRT, which showed a mean decrease of  $0.64 \pm 0.71 \mu\text{m}$  (95% CI  $-2.75$  to  $1.57$   $P = 1.0$ ).

Baseline central choroidal thickness was  $245.01 \pm 18 \mu\text{m}$  for the sham group and  $251.89 \pm 20 \mu\text{m}$  for the NRT group ( $P = 0.54$ ). Measurements remained stable throughout the follow-up for both groups, with no statistically significant changes between the groups or compared with baseline ( $233.58 \pm 15 \mu\text{m}$  vs.  $240.42 \pm 19 \mu\text{m}$  for sham and NRT, respectively,  $P = 0.53$ ). No significant clinical or statistical changes in OCT angiography for superficial vascular density have been observed in both groups during the study follow-up.

**Best-corrected visual acuity.** At the baseline, there was no statistically significant difference in BCVA between groups, and over the follow-up period, there was no statistically significant change in BCVA within each group, compared with baseline ( $P > 0.05$  for all measurements and time points) (Figure 5). However, the difference between groups did become statistically significant over time, and at 12 months, the mean BCVA was  $65.6 \pm 3.7$  (20/50) for sham and  $73.2 \pm 1.8$  letters (20/40) for NRT (mean difference of  $-7.6 \pm 3.6$ , 95% CI  $-14.7$  to  $-0.5$ ,  $P = 0.035$ ).

**Fundus automated perimetry.** Because of the lack of the fundus automated perimetry system at the beginning of the trial, this measurement was performed only at the 12-month visit. Stable and sufficient fixation was present in all patients for perimetry measurements. At that time, inner ring macular sensitivity was significantly higher in the NRT group ( $28.22 \pm 0.71$  dB) compared with sham ( $25.86 \pm 1.13$  dB,  $P = 0.028$ ) (Figure 6A). No significant difference was observed

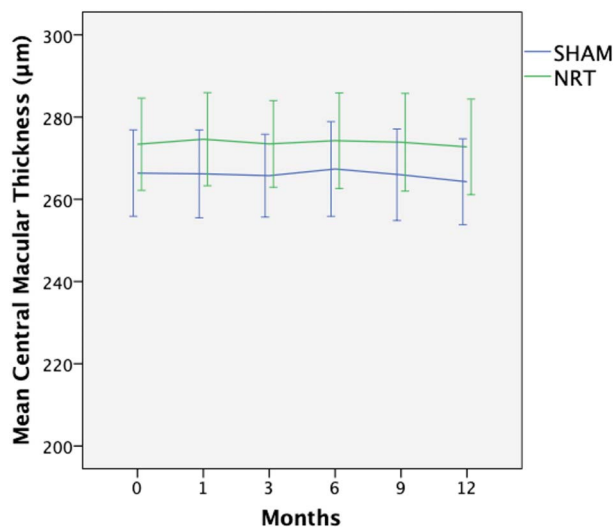


Fig. 4. Mean CMT in the NRT and sham groups over 12-month follow-up.

in the foveal and outer ring sensitivity measurements, mean deviation (MD) or pattern standard deviation (PSD) values between the groups ( $P = 0.15$ ). Total fixation area was larger in the sham group, compared with NRT ( $7.94^{o2} \pm 2.7$  vs.  $3.47^{o2} \pm 1.46$ ,  $P < 0.001$ ) (Figure 6B).

*Adverse Events*

No severe adverse events related to the treatment have been detected in both groups. No visible laser burns were found in patients treated with NRT. We did not find any laser scars by SS-OCT enface imaging or autofluorescence, and there was no decrease in retinal sensitivity in the treatment group, compared with sham at 12 months.

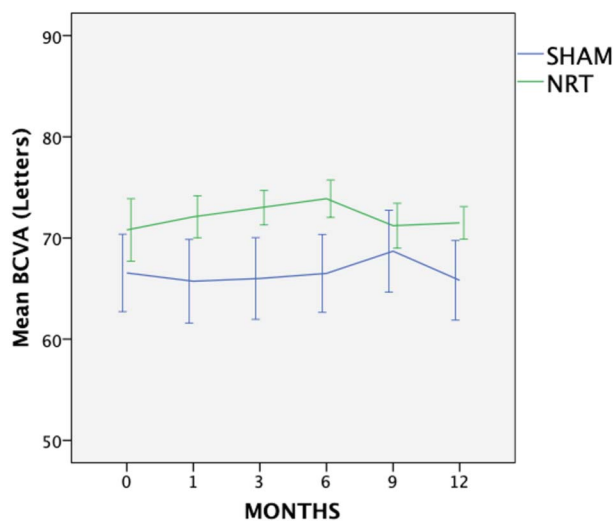
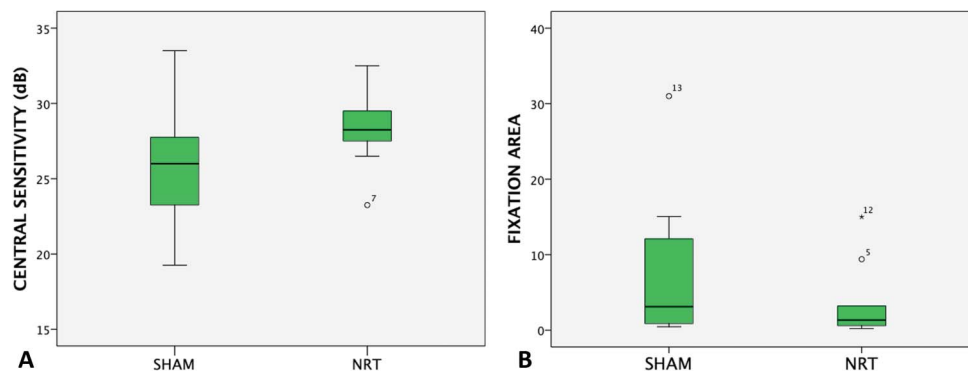


Fig. 5. Mean BCVA in NRT and sham groups over 12-month follow-up. Data shown as mean ETDRS letters.

**Fig. 6. A.** Mean central sensitivity (dB) measured by automated fundus perimetry of sham and NRT groups at 12 months. **B.** Mean fixation area ( $^{\circ 2}$ ) measured by automated fundus perimetry in NRT and sham groups. Numbers on the plots indicate individual outlier patients. \*Represents outlier value.



## Discussion

Nondamaging retinal laser therapy was safe and well tolerated in MacTel patients, and it significantly decreased the EZD area compared with sham at 12 months, which could represent a neuroprotective effect of the laser-induced hyperthermia below the tissue damage threshold. Statistically significant differences between groups in visual acuity and retinal sensitivity have been detected, suggesting the structural and functional effect within the first year of this prospective, controlled, randomized clinical trial.

Conventional laser photocoagulation has been used for decades in the treatment of several retinal diseases; however, it has not been effective for MacTel Type 2, with no significant structural or functional changes reported.<sup>20</sup> Our approach differs significantly from focal laser photocoagulation: Conventional retinal laser treatment aims at obliteration of abnormal vessels, such as microaneurism or telangiectatic capillaries, whereas NRT induces photothermal stimulation of the RPE with no visible structural damage to cells.<sup>14</sup> Because of the lack of tissue damage, NRT is applied in a very dense grid, covering the treatment zone nearly confluent, unlike the sparse focal coagulation. In addition, the absence of damage allows periodic retreatment of the retina, which is critical in the management of chronic diseases.<sup>12</sup>

For years, the therapeutic goal for MacTel was to control vascular changes and leakage observed on fluorescein angiography, which was the diagnostic system of choice. However, with better diagnostic methods, such as OCT and OCT angiography and the current hypothesis that MacTel is a neurodegenerative disease rather than a pure vascular disorder, the goal has shifted to approaches focusing on neuroprotection. Leading this strategy, the MacTel Study Group has published results of the Phase I and Phase II clinical trial using CNTF that seemed to be safe in both trials. In the Phase II trial, eyes in the sham group exhibited 31% progression in the EZD area, compared with

CNTF-treated eyes.<sup>11,21</sup> Although these results are promising, longer and larger Phase III trial data are warranted to confirm the safety and efficacy of this approach. Meanwhile, currently available methods, such as NRT, seem to be safe and, based on the results of this trial, could be used to at least halt the progressive natural history of MacTel.

Our protocol used the same parameters as in the CNTF trial for the primary outcome, which was the loss of EZ integrity, measured on high-resolution OCT enface images. This parameter was chosen as a measure of the photoreceptor loss, and it has shown a good correlation with EZ segmentation on OCT and histological characteristics of photoreceptors' inner and outer segments.<sup>22</sup> Remarkable anatomical improvements in the NRT group compared with sham correlated positively with functional results at 12 months, including higher retinal sensitivity, smaller fixation area, and better acuity in the NRT group. As shown in large observational studies, acuity decreases very slowly in MacTel patients, even with significant EZD.<sup>1</sup> These results support the structure–function relationship suggested by the CNTF trials.<sup>23</sup>

Sublethal hyperthermia of the retina induces HSP expression,<sup>24</sup> which could at least in part explain the mechanism of action leading to therapeutic benefits of NRT. Normally, HSPs and other chaperones refold damaged proteins and protect cells from their aggregation and proteotoxicity.<sup>25</sup> HSP27 and 70 have shown to provide antiapoptotic functions and prevent retinal cell death by hyperexpression of HSP70 and by hypoexpression of cleaved caspase 3 in the experimental model of tissue hyperthermia.<sup>26</sup> Therefore, increased expression of HSP and co-chaperones in the RPE in response to laser-induced thermal stress might facilitate partial restoration of the RPE function, as well as glial and retinal cells, and promote their survival.

Postmortem studies demonstrated that the deep plexus retinal vasculature is dilated in MacTel Type 2 patients, and these areas appear to have Müller cell

depletion.<sup>2</sup> Experimental ablation of Müller cells caused neuroretinal degeneration resembling some aspects of MacTel, such as photoreceptor apoptosis and vascular telangiectasis.<sup>27</sup> We have previously reported that the activation of Müller cells in and around laser lesions (observed by glial fibrillary acidic protein expression) may be responsible for retinal wound contraction and restoration of the photoreceptor layer after thermal damage.<sup>15</sup> Activation of Müller cells by NRT might be one of the mechanisms of action specifically beneficial for MacTel because it might be responsible for restoration of the EZ band seen in at least partially in three eyes from this trial (Figure 1). Spontaneous restoration of the EZ line has also been reported in clinical series<sup>28</sup>; however, in our controlled trial, we did not observe this in the sham group, where the EZD actually enlarged over time.

This study is limited because of the small number of enrolled patients and relatively short follow-up. Because of the small sample size of this trial, baseline differences mainly for EZD were evaluated by relative (%) change in EZD over time as the best feasible measure to properly compare results with a limited number of patients. However, even with a small number of patients enrolled, randomization and sham-control add confidence in its findings, compared to earlier pilot tests in a case series.<sup>12</sup> Another limitation was the availability of fundus automated perimetry measurement only at the 12-month visit; hence, we were unable to evaluate progression of the retinal sensitivity over time. We plan to keep following these patients, and we should be able to provide such comparison in the future. It is clear, however, that NRT did not cause any decrease in retinal sensitivity compared with sham eyes and normal population, which would occur with high-density photocoagulation macular grid.<sup>29,30</sup>

In conclusion, findings of our study indicate a superior short-term clinical performance of NRT over sham, based on anatomic and functional measures. These observations should constitute a “proof of principle” that the nondamaging retinal laser may have a role in the treatment of MacTel Type 2, but these data should be confirmed by longer follow-up and larger clinical trials.

**Key words:** laser, retina, macular telangiectasia type 2, PASCAL, randomized clinical trial.

## References

1. Charbel Issa P, Gillies MC, Chew EY, et al. Macular telangiectasia type 2. *Prog Retin Eye Res* 2013;34:49–77.
2. Powner MB, Gillies MC, Tretiach M, et al. Perifoveal Müller cell depletion in a case of macular telangiectasia type 2. *Ophthalmology* 2010;117:2407–2416.
3. Aldredge CD, Garretson BR. Intravitreal triamcinolone for the treatment of idiopathic juxtafoveal telangiectasis. *Retina* 2003;23:113–116.
4. Arevalo JF, Sanchez JG, Garcia RA, et al. Indocyanine-green-mediated photothrombosis (IMP) with intravitreal triamcinolone acetonide for macular edema secondary to group 2A idiopathic parafoveal telangiectasis without choroidal neovascularization: a pilot study. *Graefes Arch Clin Exp Ophthalmol* 2007;245:1673–1680.
5. Friedman SM, Mames RN, Stewart MW. Subretinal hemorrhage after grid laser photocoagulation for idiopathic juxtafoveal retinal telangiectasis. *Ophthalmic Surg* 1993;24:551–553.
6. Hussain N, Das T, Sumasri K, Ram LS. Bilateral sequential photodynamic therapy for sub-retinal neovascularization with type 2A parafoveal telangiectasis. *Am J Ophthalmol* 2005;140:333–335.
7. Lira RP, Silva VB, Cavalcanti TM, et al. Intravitreal ranibizumab as treatment for macular telangiectasia type 2. *Arch Ophthalmol* 2010;128:1075–1078.
8. Charbel Issa P, Finger RP, Kruse K, et al. Monthly ranibizumab for nonproliferative macular telangiectasia type 2: a 12-month prospective study. *Am J Ophthalmol* 2011;151:876–886.
9. Charbel Issa P, Finger RP, Holz FG, Scholl HP. Eighteen-month follow-up of intravitreal bevacizumab in type 2 idiopathic macular telangiectasia. *Br J Ophthalmol* 2008;92:941–945.
10. Toy BC, Koo E, Cukras C, et al. Treatment of nonneovascular idiopathic macular telangiectasia type 2 with intravitreal ranibizumab: results of a phase II clinical trial. *Retina* 2012;32:996–1006.
11. Chew EY, Clemons TE, Jaffe GJ, et al. Macular telangiectasia type 2-phase 2 CNTF Research group. Effect of ciliary neurotrophic factor on retinal neurodegeneration in patients with macular telangiectasia type 2: a randomized clinical trial. *Ophthalmology* 2019;126:540–549.
12. Lavinsky D, Wang J, Huie P, et al. Nondamaging retinal laser therapy: rationale and applications to the macula. *Invest Ophthalmol Vis Sci* 2016;57:2488–2500.
13. Sramek C, Mackanos M, Spitler R, et al. Non-damaging retinal phototherapy: dynamic range of heat shock protein expression. *Invest Ophthalmol Vis Sci* 2011;52:1780–1787.
14. Lavinsky D, Sramek C, Wang J, et al. Subvisible retinal laser therapy: titration algorithm and tissue response. *Retina* 2014;34:87–97.
15. Sher A, Jones BW, Huie P, et al. Restoration of retinal structure and function after selective photocoagulation. *J Neurosci* 2013;33:6800–6808.
16. Yang Z, Tatham AJ, Zangwill LM, et al. Diagnostic ability of retinal nerve fiber layer imaging by swept-source optical coherence tomography in glaucoma. *Am J Ophthalmol* 2015;159:193–201.
17. Mohler KJ, Draxinger W, Klein T, et al. Combined 60 Wide-field choroidal thickness maps and high-definition en face vasculature visualization using swept-source megahertz OCT at 1050 nm. *Invest Ophthalmol Vis Sci* 2015;55:6284–6293.
18. Zhang C, Tatham AJ, Medeiros FA, et al. Assessment of choroidal thickness in healthy and glaucomatous eyes using swept source optical coherence tomography. *PLoS One* 2014;9:e109683.
19. Montesano G, Bryan SR, Crabb DP, et al. A comparison between the compass fundus perimeter and the Humphrey field analyzer. *Ophthalmology* 2019;126:242–251.



20. Meyer-Ter-Vehn T, Herzog S, Schargus M, et al. Long-term course in type 2 idiopathic macular telangiectasia. *Graefes Arch Clin Exp Ophthalmol* 2013;251:2513–2520.
21. Chew EY, Clemons TE, Peto T, et al. Ciliary neurotrophic factor for macular telangiectasia type 2: results from a phase 1 safety trial. *Am J Ophthalmol* 2015;159:659–666.
22. Curcio CA, Messinger JD, Sloan KR, et al. Human chorioretinal layer thicknesses measured in macula-wide, high-resolution histologic sections. *Invest Ophthalmol Vis Sci* 2011;52:3943.
23. Heeren TFC, Kitka D, Florea D, et al. Longitudinal correlation of ellipsoid zone loss and functional loss in macular telangiectasia type 2. *Retina* 2018;38:S20–S26.
24. Desmettre T, Maurage CA, Mordon S. Transpupillary thermotherapy (TTT) with short duration laser exposures induce heat shock protein (HSP) hyperexpression of choroidoretinal layers. *Lasers Surg Med* 2003;33:102–107.
25. Gestwicki JE, Garza D. Protein quality control in neurodegenerative disease. *Prog Mol Biol Transl Sci* 2012;107:327–353.
26. Sun Y, Zhang S, Liao H, et al. Pre-exposure to low-power diode laser irradiation promotes cytoprotection in the rat retina. *Lasers Med Sci* 2015;30:127–133.
27. Shen W, Fruttiger M, Zhu L, et al. Conditional Muller cell ablation causes independent neuronal and vascular pathologies in a novel transgenic model. *J Neurosci* 2012;32:15715–15727.
28. Wang Q, Tuten WS, Lujan BJ, et al. Adaptive optics microperimetry and OCT images show preserved function and recovery of cone visibility in macular telangiectasia type 2 retinal lesions. *Invest Ophthalmol Vis Sci* 2015;56:778–786.
29. Midena E, Segato T, Bottin G, et al. The effect on the macular function of laser photocoagulation for diabetic macular edema. *Graefes Arch Clin Exp Ophthalmol* 1992;230:162–165.
30. Hudson C, Flanagan JG, Turner GS, et al. Influence of laser photocoagulation for clinically significant diabetic macular oedema (DMO) on short-wavelength and conventional automated perimetry. *Diabetologia* 1998;41:1283–1292.